

PLANS FOR AN AEROELASTIC PREDICTION WORKSHOP

**Jennifer Heeg^{1a}, Josef Ballmann^{2a}, Kumar Bhatia³, Eric Blades⁴,
Alexander Boucke^{2b}, Pawel Chwalowski^{1b}, Guido Dietz⁵, Earl Dowell⁶,
Jennifer Florence^{1c}, Thorsten Hansen⁷, Mori Mani⁸, Dimitri Mavriplis⁹,
Boyd Perry^{1d}, Markus Ritter¹⁰, David Schuster^{1e}, Marilyn Smith¹¹,
Paul Taylor¹², Brent Whiting¹³, and Carol Wieseman^{1f}**

¹ *NASA Langley Research Center*

Hampton, Virginia, USA

^{1a} jennifer.heeg@nasa.gov

^{1b} pawel.chwalowski@nasa.gov

^{1c} jennifer.p.florence@nasa.gov

^{1d} boyd.perry.iii@nasa.gov

^{1e} david.m.schuster@nasa.gov

^{1f} carol.c.wieseman@nasa.gov

² *Aachen University*

Aachen, Germany

^{2a} ballmann@itam-gmbh.de

^{2b} alexander.boucke@itam-gmbh.de

³ *Boeing Commercial Aircraft*

Seattle, Washington, USA

kumar.g.bhatia@boeing.com

⁴ *ATA Engineering, Inc*

Huntsville, Alabama, USA

eric.blades@ata-e.com

⁵ *European Transonic Wind tunnel*

Köln, Germany

gd@etw.de

⁶ *Duke University*

Durham, North Carolina, USA

earl.dowell@duke.edu

⁷ *ANSYS*

Otterfing, Germany

thorsten.hansen@ansys.com

⁸ *Boeing Research & Technology*

St. Louis, Missouri, USA

mori.mani@boeing.com

⁹ *University of Wyoming*

Laramie, Wyoming, USA

Mavripl@uwyo.edu

¹⁰ *Deutsches Zentrum für Luft- und Raumfahrt*

Göttingen, Germany

markus.ritter@dlr.de

¹¹ *Georgia Institute of Technology*

Atlanta, Georgia, USA

marilyn.smith@aerospace.gatech.edu

¹² *Gulfstream Aerospace*

Savannah, Georgia, USA

paul.taylor@gulfstream.com

¹³ *Boeing Research & Technology*

Seattle, Washington, USA

brent.a.whiting@boeing.com

Keywords: validation, workshop, computational aeroelasticity, HIRENASD, RSW, BSCW

Abstract: This paper summarizes the plans for the first Aeroelastic Prediction Workshop. The workshop is designed to assess the state of the art of computational methods for predicting unsteady flow fields and aeroelastic response. The goals are to provide an impartial forum to evaluate the effectiveness of existing computer codes and modeling techniques, and to identify computational and experimental areas needing additional research and development. Three subject configurations have been chosen from existing wind tunnel data sets where there is pertinent experimental data available for comparison. For each case chosen, the wind tunnel testing was conducted using forced oscillation of the model at specified frequencies.

NOMENCLATURE

| | | | |
|-----------|--|------------|--|
| b | Model span | x | Chordwise location |
| c_{ref} | Model reference chord | y | Spanwise location |
| C_p | Pressure coefficient | y^+ | Dimensionless wall distance in boundary layer modeling |
| f | Frequency of excitation, Hz | Δy | Normal spacing of the 1 st cell at the viscous wall |
| M | Freestream Mach number | α | Angle of attack, mean position |
| q | Freestream dynamic pressure | θ | Amplitude of pitch oscillation |
| Re_c | Reynolds number based on reference chord | | |

1 INTRODUCTION

Credibility of computational methods has improved in recent years, in large part due to dedicated verification and validation efforts. Relying on definitions established by the Department of Energy^{1,2} and the AIAA^{3,4,5}: validation is the process of determining how well the results from a computational model compare with the characteristics of the physical system of interest.

Participants in the Drag Prediction Workshop (DPW)⁶ series and the High Lift Prediction Workshop⁷ have performed quantitative and qualitative assessments of a significant cross-section of computational methods, relative to experimental data. These efforts have been used to determine the level of confidence that can be placed in computational results, focusing on steady state rigid configurations. The Aeroelastic Prediction Workshop (AePW) has been crafted to follow in the footsteps of these prior workshops, extending validation efforts to unsteady computational methods and coupled fluid/structure methods.

The accuracy required from an aeroelastic calculation depends on the intended usage of the information; the level of detail of the physics required to be captured to achieve the required accuracy depends on the phenomena of interest. The requirements for capturing static aeroelastic phenomena are generally more modest than those required for capturing dynamic aeroelastic phenomena; those associated with linear behavior have more modest requirements than those of a system with significant nonlinear behavior.

Validation data sets and validation analyses are different from phenomenological investigations. There have been noteworthy efforts in aeroelastic validation, including recent work by Green and colleagues,⁸ which was funded by the U.S. Air Force Institute for High Performance Computing. In their work, five Navier-Stokes flow solvers were used to evaluate the unsteady aeroelastic predictions for five 2-D validation cases. The eventual goal was prediction of unsteady flow over a fighter aircraft with stores in captive carriage. Due to resource constraints and technical redirection, however, only preliminary steps have been taken towards achieving this goal.

There are also notable publications detailing developments within the field of computational aeroelasticity that can be used to provide guidance in determining the critical areas of interest for validation efforts.^{9, 10, 11} These references and other survey papers indicate that levels of aerodynamic modeling- e.g., strip theory, panel methods, Euler equations and Navier Stokes equations- have been used with varying degrees of success to predict static and dynamic

aeroelastic properties of configurations of varying complexity. The subsonic flow range properties are thought to be well-predicted by current methods, but the definition of “well-predicted” and the Mach number range for “good enough” agreement are phenomenon-dependent as well as end-usage-dependent. This workshop series aspires to provide a forum for unbiased and quantitative evaluation of different complexities, including flow phenomena, equation complexity, aeroelastic coupling strength, and configuration complexities.

2 OBJECTIVES

The objective in conducting workshops on aeroelastic prediction is to assess state-of-the-art Computational Aeroelasticity (CAE) methods as practical tools for the prediction of static and dynamic aeroelastic phenomena. No comprehensive aeroelastic benchmarking validation standard currently exists, greatly hindering validation objectives.

The AGARD 445.6 wing¹², tested in 1960, provides one of the most studied configurations, and has been previously viewed as a benchmark. The data set, however, lacks the details necessary for validating modern computational codes. There are no surface pressure, structural displacement or unsteady flow field measurements. For each high-fidelity analysis that can be run, the experiment comparison data is limited to the flutter dynamic pressure and dominant frequency at the destabilizing condition.

The approach being taken in conducting the planned first aeroelastic prediction workshop is to perform comparative computational studies on selected test cases. The workshop effort will utilize existing experimental data sets and a building block approach to validate aspects of CAE tools that can be addressed through these existing data sets. Through the exercise of existing data sets, the workshop will help to identify requirements for additional validation experiments. The workshop activities will further refine the definitions of what constitutes a “good validation data set” for computational aeroelasticity. Additional code development activities required to adequately predict aeroelastic phenomena will also be identified.

Quantitative assessment, along with qualitative statements and recommendations, are essential objectives of a proposed series of workshops. Quantifying and identifying the sources of errors and uncertainties associated with the computational methods are central principles to advancing the state of the art. Developing experimental databases suitable for validation will result in accuracy improvements in computational methods. Desired outcomes of this workshop activity include identifying the most fertile areas for methodology improvement and development along with defining the experiments necessary to validate existing and developing methods. Compilation and detailing of lessons learned is also essential to accomplishing these outcomes.

3 VALIDATION STRATEGY

The AIAA Committee on Standards for Computational Fluid Dynamics has generated a guide for verification and validation. Quoting from reference 5:

“The fundamental strategy of validation is the identification and quantification of error and uncertainty in conceptual and computational models. The recommended validation method is to employ a building-block approach. This approach divides the

complex engineering system of interest into ... progressively simpler phases ... The strategy in this approach is the assessment of how accurately the computational results compare with experimental data, with quantified uncertainty estimates, at multiple levels of complexity. Each phase of the process represents a different level of flow physics coupling and geometrical complexity.”

The validation strategy to be employed in this proposed workshop series follows these recommendations, dividing the complex problem of nonlinear unsteady aeroelastic analysis of an aerospace vehicle into simpler components. Each component, or building block, is formulated to isolate a specific aspect of the problem in a way that the contributing physics can be thoroughly investigated.

The validation strategy for the Aeroelastic Prediction Workshop series is to divide aeroelastic phenomena into the classically identified component parts and then further subdivide these parts into smaller blocks, each with particular limits on the behavior or physical phenomena. The choices of building blocks to include in the first workshop are driven by several criteria. The first criterion applied is the existence of a compatible and sufficient experimental data set. The second criterion applied for the initial workshop effort is simplicity, both of configuration and phenomena. The number of independent variables strongly affecting an aeroelastic problem quickly becomes overwhelming, eliminating the ability to identify the source of variations or errors. Phenomenologically, we choose to begin with moderately simple flow fields and moderately simple geometries and structures.

The coarse-grain building blocks in aeroelasticity are: 1) unsteady aerodynamics; 2) structural dynamics; and 3) coupling between the fluid and the structure. In this first workshop, we focus primarily on validating unsteady aerodynamic models and methods, with an initial venture into weakly coupled aeroelastic models.

3.1 Aerodynamic building blocks

There is an extensive range of unsteady flow physics that could be considered and broken into building blocks. In this first workshop, we have chosen to focus on transonic conditions for several reasons. Transonic conditions are often considered to be the most critical conditions with regard to aeroelastic phenomena such as flutter onset, buffet and limit cycle oscillations. In the transonic range, various flow phenomena can initiate and produce severe aeroelastic issues. As such, the most significant disagreements among computational results and between computations and experiments are observed at transonic conditions. Coupling the criticality of the computation with the complexity of the computation draws our attention to understanding the variability and errors associated with transonic predictions as the starting point for the workshop series.

Consequently, predictions of fully turbulent transonic flow will serve as the starting point for the initial workshop efforts. Experimentally, initial test cases were selected where boundary layer trip strips artificially forced transition. It is thought that this selection will help eliminate laminar to turbulent transition as a source of variation between the experiment and the turbulent flow calculations.

Within the transonic range, the physics can include shocks of varying strength and position, as well as separated flow regions. The flow physics building blocks will be generated with test

cases having weak shocks and attached flow progressing through test cases with strong shocks and separated flow to test cases with strong shocks and alternating separated and attached flow. Ideally, this test case progression will build confidence in the ability to predict phenomena of increasing complexity.

Perhaps the most demanding aeroelastic phenomenon for unsteady aerodynamic prediction is buffet. Similar physical phenomena, including abrupt wing stall and non-synchronous vibration in turbomachinery flows, are similarly difficult to predict. In all of these cases, the aerodynamic flow itself may become unstable even in the absence of any structural motion. Once the flow becomes unstable and begins to fluctuate, it drives structural motion. Further, if the frequency of the buffeting flow coincides or nearly coincides with a structural frequency, then large structural motions may occur. Currently, buffet is perhaps the most poorly understood of all unsteady aerodynamic phenomena and thus is not a focus of the present workshop, consistent with our building block approach. An aspiration of this workshop series is to assess and advance computational aeroelastic capabilities to address this complex phenomenon.

Characterizing the important aerodynamic features for aeroelastic computations is divided by exclusion or inclusion of time dependence of the solutions. In this workshop, the steady or static solutions will be briefly addressed as building blocks toward the dynamic solutions. Many important aeroelastic phenomena are time-dependent, requiring that computational methods operate in a time-accurate manner.

3.2 Structural dynamic building blocks

The building blocks required for the structural and structural dynamic validation will not be discussed in detail in this document due to the aerodynamic focus of the initial workshop. Isolating and assessing the variability in the structural portion of the problem can be further divided into static validation efforts, loads with increasing frequency, loads with increasingly complex distribution, loads with increasingly complex time dependence, response of a system with closely spaced modes, response of a system with significant structural and geometric nonlinearities, and potentially many other building blocks. For the initial workshop, the test cases are selected based on criteria that reduce the significance of structural variations.

3.3 Fluid / structure coupling building blocks

The degree of coupling between the fluid and the structure is dependent on many variables: flow field force distribution (pressure distribution); flow field strength (dynamic pressure); geometric presentation of the structure to the flow field (deformation distribution); and magnitude of the deformation.

For the aerodynamic problem to be completely uncoupled from the structural considerations, the structure must be perfectly rigid, without any elastic deformation. This is an idealization, as all real structures are flexible under loading. Weakly coupled systems are designated as those systems that have small influences of the structural deformation on the aerodynamics, or small influences of the aerodynamics on the structure. Models which are built to be rigid are classified as weakly coupled. Most aerodynamic studies assume that the model is completely rigid and

neglect all influence of the structural motion. This idealization is applied to the majority of steady aerodynamic analyses.

4 FIRST WORKSHOP PLAN OF ACTION

The first workshop challenges the computational community to apply best practices and state-of-the-art methods and codes to predict unsteady aerodynamic characteristics for rigid or weakly coupled aeroelastic systems. Within this scope, the test cases have been laid out in building blocks of increasing complexity.

Very thoughtful deliberation of phenomena and complexity was the primary driver for the selection of test cases for the first workshop. Consideration of the building blocks of a computational aeroelastic validation effort was key in this deliberation. This dissection allowed for the wider consideration of configurations and data sets. The breadth of test cases is a by-product of the diversity of the workshop organizing committee, in terms of resources, configuration interest and confidence in current methodologies.

The test configurations and conditions were selected in an attempt to advance in complexity from fully turbulent with attached flow and weak shocks to transient separation conditions with strong shocks and significant interactions between these flow features.

The workshop will employ three configurations: the Rectangular Supercritical Wing (RSW) model, the Benchmark SuperCritical Wing (BSCW) model, and the High Reynolds Number Aero-Structural Dynamics (HIRENASD) model. The rationale for each of these selections is tied to the building block approach previously discussed. The matrix of test cases is outlined below. Analysts may choose to provide calculations for any combination of the configurations shown in the outline.

For each configuration to be analyzed, results from three studies are required: a convergence study, steady analysis and time-accurate response due to forced oscillations. Validation is accomplished by comparison with wind tunnel test data. Reference quantities for the validation comparisons are given in Table 1.

1. Rectangular Supercritical Wing: ($M=0.825$, $Re_c=4.0$ million, test medium: R-12)
 - a) Steady Cases
 - i. $\alpha = 2^\circ$ (RTO Case 6E23, TDT pt. 626)
 - ii. $\alpha = 4^\circ$ (RTO Case 6E24, TDT pt. 624)
 - b) Dynamic Cases
 - i. $\alpha = 2^\circ$, $\theta = 1.0^\circ$, $f = 10$ Hz. (RTO Case 6E54, TDT pt. 632)
 - ii. $\alpha = 2^\circ$, $\theta = 1.0^\circ$, $f = 20$ Hz. (RTO Case 6E56, TDT pt. 634)
2. Benchmark SuperCritical Wing (Semi-Blind) ($M=0.85$, $Re_c=4.49$ million, test medium: R-134a)
 - a) Steady Case
 - i. $\alpha = 5^\circ$
 - b) Dynamic Cases
 - i. $\alpha = 5^\circ$, $\theta = 1^\circ$, $f = 1$ Hz

- ii. $\alpha = 5^\circ, \theta = 1^\circ, f = 10 \text{ Hz}$
- 3. HIRENASD ($M = 0.80$, test medium: nitrogen)
 - a) Steady (Static Aeroelastic) Cases
 - i. $Re_c = 7.0 \text{ million}, \alpha = 1.5^\circ$, static aeroelastic, (exp. 132)
 - ii. $Re_c = 23.5 \text{ million}, \alpha = -1.34^\circ$, static aeroelastic, (exp. 250)
 - b) Dynamic Cases: forced oscillation at 2nd Bending mode frequency
 - i. $Re_c = 7.0 \text{ million}, \alpha = 1.5^\circ, f = 78.9 \text{ Hz}$ (exp. 159)
 - ii. $Re_c = 23.5 \text{ million}, \alpha = -1.34^\circ, f = 80.3 \text{ Hz}$ (exp. 271)

Table 1. Reference quantities.

| | | RSW | BSCW | HIRENASD |
|--|-----------|----------------------|---------------------|---|
| Reference chord | c_{ref} | 24 inches | 16 inches | 0.3445 m |
| Model span | b | 48 inches | 32 inches | 1.28571 m |
| Area | A | 1152 in ² | 512 in ² | 0.3926 m ² |
| Dynamic pressure | q | 108.9 psf | 200 psf | 40.055 kPa (pt 159,132) 88.697 kPa (pt 271,250) |
| Moment reference point, relative to axis system shown in Figs 2, 5 and 9 | \bar{x} | 11.04 inches | 4.8 inches | 0.252 m |
| | \bar{y} | 0 | 0 | -0.610 m |
| | \bar{z} | 0 | 0 | 0 |
| Transfer function reference quantity | | Pitch angle | Pitch angle | Vertical displacement (at $x=1.24521\text{m}$, $y=0.87303\text{m}$) |

5 CONFIGURATIONS & TEST CASES FOR THE FIRST WORKSHOP

The workshop will employ three configurations, each of which is detailed below. For each configuration, there is at least one steady case and a corresponding dynamic case. The dynamic cases are all responses due to forced oscillations. The first two configurations and selected test cases have forcing frequencies that are well separated from the aeroelastic modes. Two rectangular wings, RSW and BSCW, with supercritical airfoil sections and assumed rigid structures provide these entry-level configurations. The second configuration, the BSCW, also serves as a semi-blind test case.

The third configuration, HIRENASD, is a semi-span model that was tested with sinusoidal excitations at frequencies near the aeroelastic modal frequencies. For this workshop, cases where the forcing frequency is coincident with the second bending mode frequency of the wing are analyzed. The HIRENASD experimental data set contains significantly more sensor data than the rectangular wings' data sets.

5.1 Test configuration 1: Rectangular Supercritical Wing

The Rectangular Supercritical Wing (RSW) was chosen as the configuration for the first test

case. This model was tested in the NASA Langley Transonic Dynamics Tunnel (TDT) in 1983, as shown Figure 1, and detailed in references 13, 14, 15 and 16. The test medium used was R-12 Freon. The TDT has slotted test section walls; the slots were open for the data acquired during RSW testing.

The RSW is a rectangular planform wing as shown in Figure 2, with a 12% thick supercritical airfoil that is depicted in Figure 3 (red dashed line). The wing was mounted to a small splitter plate, offset 6 inches from the wind tunnel wall. The model was designed with the goal of being structurally rigid; the first bending mode has a frequency of 34.8 Hz. The model’s instrumentation consists of chordwise rows of unsteady pressure sensors at 4 span stations.



Figure 1. RSW mounted in TDT.

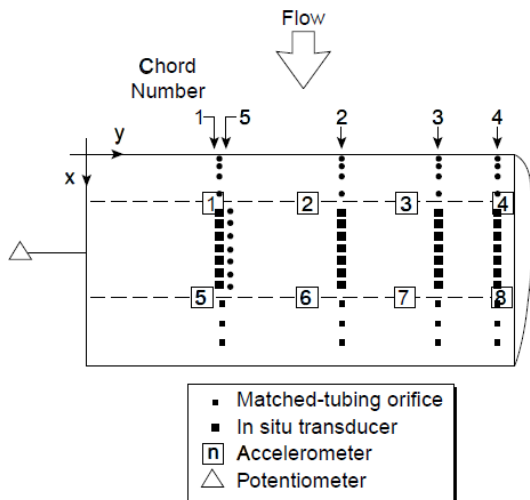


Figure 2. RSW planform view.

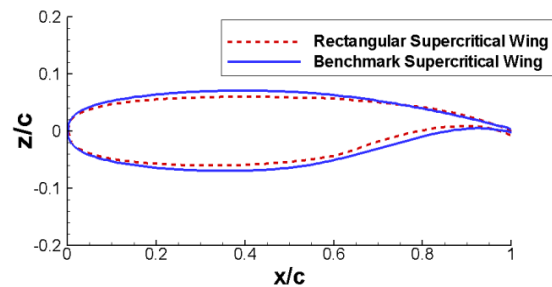


Figure 3. Airfoil sections for RSW and BSCW.

Steady data was obtained with the model held at a fixed angle of attack. Separate dynamic data was acquired by oscillating the model in a pitching motion about the 46% chord line. Testing was primarily conducted without a boundary layer transition strip, allowing natural transition from laminar to turbulent flow. In the current validation effort, we will utilize experimental data acquired with the transition point fixed; the experimental comparison data was acquired with a boundary layer transition strip at 6% chord. Analysts can make the assumption of fully turbulent flow or fixed transition point, according to their analysis capabilities. All data to be used in this study was obtained nominally at Mach 0.825, 4 million Reynolds number based on wing chord.

The test cases which have been selected for the AePW consist of two steady data sets and two dynamic data sets. The two static test cases associated with this configuration are chosen to focus on the steady solutions and their variations. The 2 degree angle of attack case is anticipated to produce a moderate-strength shock with some potential for shock-separated flow. The second static condition, 4 degrees angle of attack, is anticipated to produce a strong shock with greater potential for shock-separated flow.

The forced oscillation test cases permit the examination of the unsteady aerodynamic predictions and their variations. The static parameters associated with the test cases match those of the first static analysis test case, 2 degree angle of attack. Two forced pitch oscillation frequencies of 10 and 20 Hz allow evaluation of the methods' abilities to distinguish frequency effects. Frequency separation between the structural dynamic modes and the excitation forcing function is used to minimize the coupling of the aerodynamics and the structural dynamics. The non-zero mean angle of attack introduces a wing loading bias for which code-to-code comparisons can be made.

The steady and unsteady data was originally published as a NASA Technical Memorandum¹² and later included in an appendix to Compendium of Aerodynamic Measurements in AGARD Report 702¹⁷ and RTO TR-26¹⁸. The RSW experimental data has been widely published. Unfortunately, the only available data is the published data. It consists of mean pressures for static cases and complex pressures for forced oscillation runs. The model is unavailable for retesting or inspection, although the splitter plate has been located and its geometry has been measured for use in grid generation.

5.2 Test configuration 2: Benchmark SuperCritical Wing

The Benchmark SuperCritical Wing (BSCW), shown in Figure 4, was tested in the TDT in R-134a test medium. The model was mounted to a large splitter plate, sufficiently offset from the wind tunnel wall (40 inches) to be outside of any tunnel wall boundary layer¹⁹. The testing was conducted with the sidewall slots closed. The BSCW has a rectangular planform as shown in Figure 5, with a NASA SC(2)-0414 airfoil, shown in Figure 3 (blue solid line). The model was designed with the goal of being rigid; the spanwise first bending mode has a frequency of 24.1 Hz, the in-plane first bending mode has a frequency of 27.0 Hz and the first torsion mode has a frequency of 79.9 Hz. The model's instrumentation is limited to one row of 40 in-situ unsteady pressure transducers at the 60% span station. Boundary layer transition was fixed at 7.5% chord using size 30 grit. All data to be used in this study was obtained at Mach 0.85 and a dynamic pressure of 200 psf, fixing the Reynolds number at 4.49 million based on wing chord. Dynamic data was obtained for the BSCW by oscillating the model in a pitching motion about the 30% chord. Steady information pertinent to this configuration is calculated as the mean value from the oscillatory time histories. The data processing performed shows small variations in the mean data due to the forcing frequency. These variations will be treated as uncertainties in the steady experimental information.

This configuration was chosen because the experiment exhibited highly nonlinear unsteady behavior, specifically shock-separated transient flow. While there are fewer pressure measurements than for the RSW configuration, the time history data records are available for all test conditions. The model is also available for inspection and retesting if desired. The engineers

who conducted the testing are also available for consultation regarding the model, test conditions, data content and other insights.

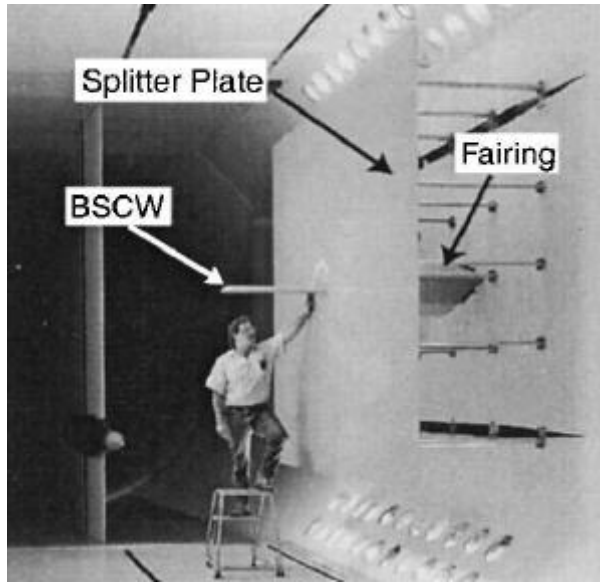


Figure 4. BSCW mounted in TDT.

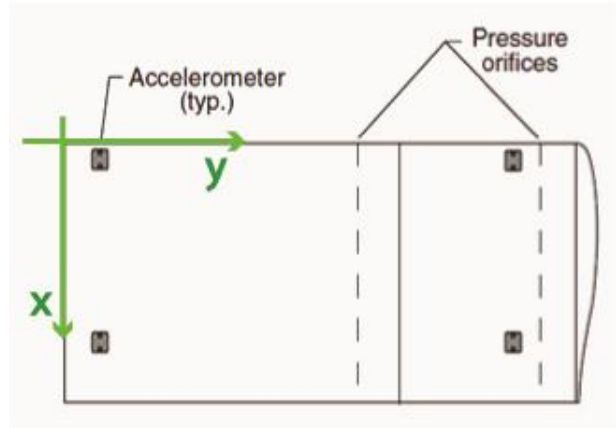


Figure 5. BSCW planform view.

The BSCW experimental data has not been widely published. It was obtained during check-out testing of the TDT Oscillating Turntable (OTT) hardware and thus was not the focus of a computational research project. While the data is publicly available in graphical form²⁰, it is viewed as obscure enough to serve as the basis for a semi-blind test case. The data sets that are available in publications are shown in Figure 6 and Figure 7.

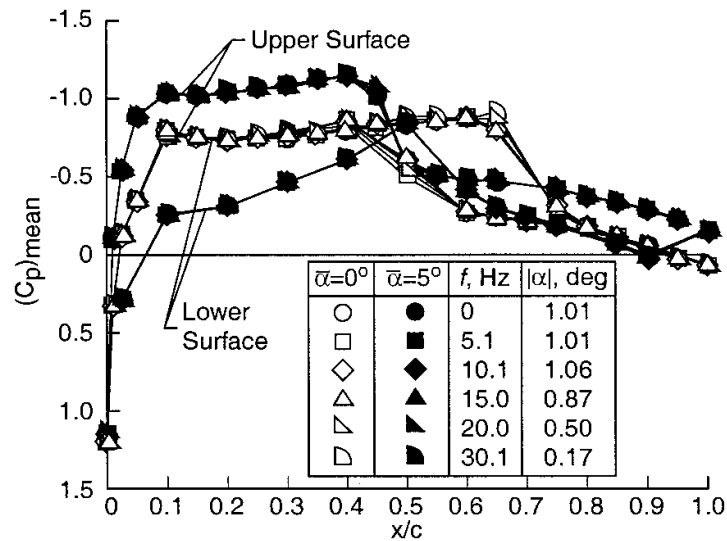


Figure 6. BSCW mean pressure coefficients, reference 20.

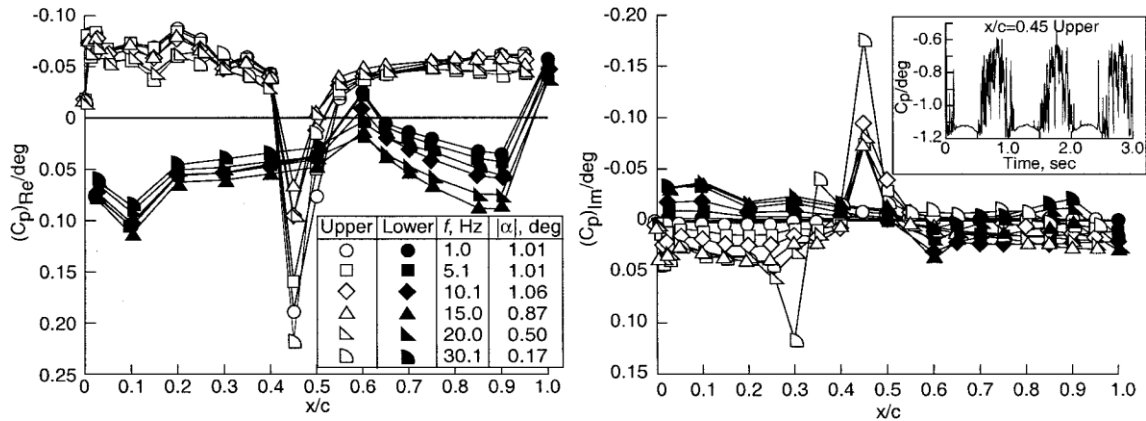


Figure 7. BSCW real and imaginary pressure coefficients at $\alpha=5$ deg for $M= 0.85$, $q= 200$ psf, and $Re_c = 4.49$ million, reference 20.

5.3 Test configuration 3: HIRENASD

The High Reynolds Number Aero-Structural Dynamics (HIRENASD) model was tested in the European Transonic Wind tunnel (ETW) in 2007, shown in Figure 8, and described by references 21, 22 and 23. The model has a 34 degree aft-swept, tapered clean wing, with a BAC 3-11 supercritical airfoil profile. The test article is a semi-span model, ceiling-mounted through a non-contacting fuselage fairing to a turntable, balance and excitation system, shown in Figure 9. The model and balance were designed to be very stiff, with well-separated modes. The first two bending modes have frequencies of approximately 27 and 79 Hz; the first torsion mode has a frequency of approximately 265 Hz. The model’s instrumentation includes 259 in-situ unsteady pressure transducers at 7 span stations. In addition to the unsteady pressures, balance measurements and accelerations were obtained. For a small set of data points, wing displacements were also extracted via stereo pattern tracking.



Figure 8. HIRENASD installed in ETW.

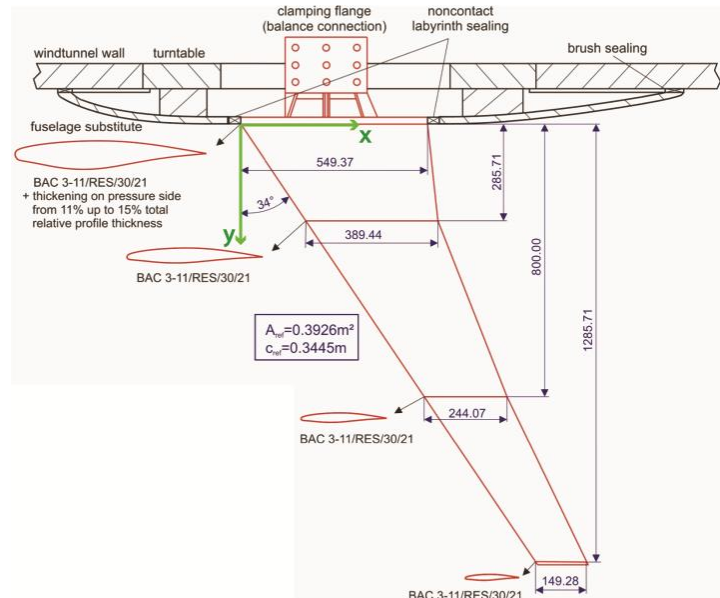


Figure 9. HIRENASD planform view; dimensions shown are in mm unless otherwise noted.

Two types of testing were conducted: angle-of-attack polars and forced oscillations. The angle-of-attack polar data was obtained by slowly varying the angle of attack at an angular sweep rate of 0.2 degrees/second, holding all other operational parameters constant. This data will be utilized primarily to provide static pressure distributions at a given test condition. The forced oscillation data was obtained by differential forcing at a specified modal frequency. All forced oscillation data to be used in the current workshop was excited near the second bending modal frequency. For all workshop test case conditions, boundary layer transition strips were affixed to the upper wing surface at 12-15% chord and to the lower surface at 5% chord. Two Reynolds numbers, 7.0 million and 23.5 million based on reference chord, will be analyzed. For all cases, the Mach number is fixed at 0.80. The lower Reynolds number case has an angle of attack of 1.5 degrees, while a more challenging angle of attack of -1.34 degrees, corresponding to the zero-lift condition, has been selected for analysis at the higher Reynolds number. All tests were conducted with nitrogen as the test medium.

The HIRENASD model was chosen as the initial coupled aeroelastic analysis configuration. The high stiffness and modal spacing produces weak aeroelastic coupling, making it a good entry-level basis of evaluation. The additional benefits of this data set are availability of time histories and expertise from the experimenters who are part of this workshop team.

Portions of the HIRENASD data set have been publicized and distributed, and the first proposed test case has already been investigated by several analysts.^{23, 24, 25, 26, 27} Availability and familiarity of the test case are viewed as benefits for easing initial comparisons. Other portions of the HIRENASD data set have not yet been published. The existing data sets available for the HIRENASD configuration are much more extensive than those listed for consideration in this workshop or previously published. The extended data set includes points that are considered to be phenomenologically more complex than the points chosen for this initial foray. Thus, this configuration has excellent potential for blind validation efforts planned beyond the first workshop.

6 ANALYSIS BUILDING BLOCKS

6.1 Geometry files

Engineers at NASA Langley have prepared IGES files of the RSW, BSCW, and HIRENASD configurations. The IGES files of the RSW (shown in Figure 10) and BSCW models were constructed from the measured data and also include splitter plate geometries. However, the splitter plates are not required to be included in the computational models.

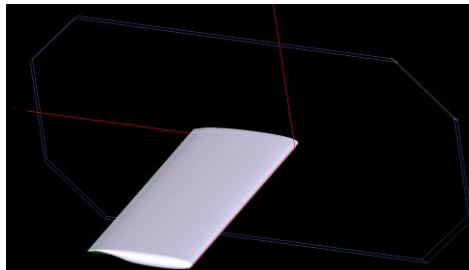


Figure 10. RSW wing IGES surface created from the measured data and the outline of the splitter plate.

6.2 Computational meshes

Five mesh types for each configuration to be analyzed at AePW will be provided to the participants, and will include: four unstructured grids and one multiblock structured grid. The four unstructured grids will consist of two sets of meshes suitable for node-based solvers, and two sets of meshes designed for cell-centered solvers. This is due to the fact that node based solvers require higher density grids than cell-centered solvers for equivalent accuracy. Each set of unstructured grids will further consist of a fully tetrahedral version and a hybrid prismatic-tetrahedral version of the same grid, where the highly stretched tetrahedra in boundary layer regions are merged into prismatic layer elements. A suite of coarse, medium and fine grids will be generated for each configuration. For those participants who wish to build their own grids, the IGES files will be available. However, participants who choose to develop their own grids are required to make them available to the AePW organizing committee to ensure that they adhere to the gridding guidelines and to ensure a comparable cross-correlation with other computational methods. This requirement is based on experience from previous workshops in order to enable duplication and further investigation of submitted workshop results. Additionally, an important workshop outcome is the generation of a large database of computational meshes that can be downloaded and used for validation studies for years to come.

6.3 Gridding guidelines

For consistency, all grids used for AePW calculations should conform to the following set of gridding guidelines listed in this section. These gridding guidelines for the Aeroelastic Prediction Workshop are adopted from the guidelines developed for the Drag Prediction Workshop and the High Lift Prediction Workshop; see Appendix I for corresponding internet addresses. These guidelines have remained relatively unchanged over the course of these previous workshops and codify much of the collective experience of the applied CFD community in aerodynamic grid generation practices. Grid-related issues' effects on drag prediction error gleaned from the experiences of DPW are summarized in reference 28. For the current workshop, a sequence of coarse, medium and fine grids are required for each configuration and the guidelines can be summarized as follows:

1. RSW initial spacing normal to all viscous walls ($Re_c = 4M$ based on $c_{ref} = 24''$)
 - a. Coarse: $y^+ \sim 1.0$, $\Delta y = 0.000083''$
 - b. Medium: $y^+ \sim 2/3$, $\Delta y = 0.000055''$
 - c. Fine: $y^+ \sim 4/9$, $\Delta y = 0.000037''$
2. BSCW initial spacing normal to all walls ($Re_c = 4.49M$ based on $c_{ref} = 16''$)
 - a. Coarse: $y^+ \sim 1.0$, $\Delta y = 0.000063''$
 - b. Medium: $y^+ \sim 2/3$, $\Delta y = 0.000042''$
 - c. Fine: $y^+ \sim 4/9$, $\Delta y = 0.000028''$
3. HIRENASD wing initial spacing normal to all walls ($Re_c = 23.5M$ based on $c_{ref} = 0.3445$ m)

Note: Same grids to be used for $Re_c = 7M$ and $Re_c = 23.5M$ cases.

 - a. Coarse: $y^+ \sim 1.0$, $\Delta y = 4.40961e-7$ m
 - b. Medium: $y^+ \sim 2/3$, $\Delta y = 2.93973e-7$ m

- c. Fine: $y^+ \sim 4/9$, $\Delta y = 1.95982e-7$ m
- 4. Normal growth rate for cells in boundary layer region < 1.25 .
- 5. Structured grids will have at least 2 cell layers of constant spacing normal to viscous walls.
- 6. Farfield will be located at $\sim 100 c_{ref}$ for all grids.
- 7. Local spacings on medium grid:
 - a. Chordwise spacing for wing leading and trailing edges $\sim 0.1\%$ local chord
 - b. Wing spanwise spacing at root and at tip $\sim 0.1\%$ local semispan
 - c. Cell size near fuselage nose and aftbody $\sim 2\% c_{ref}$
- 8. Wing trailing edge: minimum 4, 6 and 9 cells for coarse, medium and fine grids, respectively.
- 9. Grid family:
 - a. Medium mesh representative of current engineering practice
 - b. Maintain a parametric family of uniformly refined grids in sequence
 - c. Grid size to grow $\sim 3X$ for each level of refinement [structured 1.5X in I,J,K directions]
 - d. Give consideration to multigridable dimensions on structured meshes
 - e. Sample sizes: coarse: 3M, medium: 10M, fine 30M

Special effort is required to ensure that sequences of coarse, medium and fine meshes constitute a consistent “family” of grids suitable for a grid convergence study. This entails the preservation of mesh topology, stretching factors, and local variations in resolution as much as possible between grids of the same sequence. The mesh spacing specifications given for the medium grid are to be scaled appropriately for the coarse and fine grids. The given grid sizes are only estimates based on the objective that the medium grid should be representative of current engineering practice enabling a solution on mid-range computational hardware in reasonable turnaround time (i.e. considerably less than 24 hours). For unstructured grids designed for vertex-based solvers, the spacing refers to inter-nodal spacing and the resulting grid sizes are expected to be similar to the structured grid sizes. For unstructured grids for cell-centered solvers, the spacing refers to spacing between cell centers (or surface face centers), which corresponds approximately to a factor of 2 reduction in the overall number of surface points compared to the nodal solver case for a triangular surface grid. For a tetrahedral cell-centered solver mesh, the total number of grid points will be approximately 1/3 of those in node based solver mesh.

6.4 Structural models

The finite element model (FEM) of the HIRENASD configuration contains more than 200,000 uniform solid hexagonal elements, Figure 11. For modal-based solvers, the interpolation of structural modes onto surface grids is accomplished using methods detailed in reference 29. Three levels of structural model are available for workshop participants: a detailed FEM, the FEM-extracted modal definition, and the mode shapes interpolated onto the provided grids.

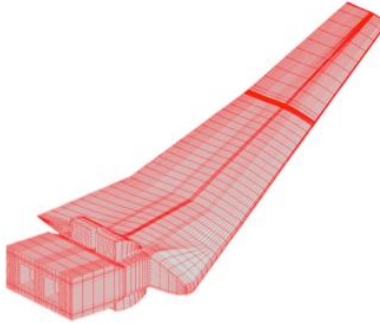


Figure 11 HIRENASD finite element model

7 WORKSHOP LOGISTICS

The first AePW will be held in conjunction with the 53rd AIAA/ASME/ASCE/AHS/ASC Structures, Structural Dynamics and Materials Conference to be held in Honolulu, Hawaii. The workshop will occur during the weekend prior to the conference, April 21-22, 2012. The AIAA Structural Dynamics Technical Committee is sponsoring this activity. The workshop is open to participants worldwide and will include representation from industry, academia and government laboratories. Participation in the aeroelastic prediction studies is not required to attend the workshop.

Workshop study participants are expected to give presentations of their results and provide data to the organizing committee. The submitted data sets and corresponding experimental data will be statistically analyzed and the results will be shared with the participants. There are no written papers associated with this workshop; the presentations are not official AIAA presentations. Presentation of results at the workshop requires submission of a micro-abstract. Details of the submission requirements are provided in Appendix II and are available on the workshop website.

The workshop will include open forums, designed to encourage transparent discussion of results and processes, promote best practices and collaborations, and develop analysis guidelines and lessons learned.

8 COMPARATIVE DATA

The workshop environment of the AePW is intended to allow a more informal discussion of details of the computational and experimental data. Individual analysts are encouraged to present and discuss their results to illustrate all features that appear and all lessons that they learn during the course of their individual investigations. It is also desirable to have direct comparisons among the computational results and with the experimental data, and to quantitatively analyze these comparative data sets. To this latter end, specific subsets of the results are required to be submitted. Those data sets are detailed below.

The required data submissions are separated into three categories: convergence study results, static analysis results and dynamic analysis results. Table 2 summarizes the required data for each of the configurations. While each analyst may choose to examine any of the configurations,

it is required that a grid convergence study be performed for each configuration for which they are submitting results. Grid convergence results are required for both the steady and dynamic analyses. For the steady case, the convergence results should be shown as the integrated load coefficients (lift coefficient, pitching moment coefficient and drag coefficient) as functions of $N^{-2/3}$, where N is the number of grid points in the analysis. The convergence criteria for the dynamic analysis will be further defined by the organizing committee.

Table 2. Comparative data submissions.

| CONFIGURATION | REQUIRED CALCULATIONS | | |
|--|--------------------------------|---|---|
| | GRID CONVERGENCE STUDIES | STEADY CALCULATIONS | DYNAMIC CALCULATIONS |
| Steady-Rigid Cases (RSW, BSCW) | C_L, C_D, C_M vs. $N^{-2/3}$ | <ul style="list-style-type: none"> • Mean C_p vs. x/c • Means of C_L, C_D, C_M | |
| Static-Aeroelastic Cases (HIRENASD) | C_L, C_D, C_M vs. $N^{-2/3}$ | <ul style="list-style-type: none"> • Mean C_p vs. x/c • Vertical displacement vs. x/c • Twist angle vs. x/c • Means of C_L, C_D, C_M | |
| Forced Oscillation Cases (all configurations) | TBD | | <ul style="list-style-type: none"> • Magnitude and Phase of C_p vs. x/c at span stations corresponding to transducer locations • Magnitude and Phase of C_L, C_D, C_M at excitation frequency • Time history of C_p at each span station for 3 pressure transducer locations |

Static analysis results should include the pressure coefficient distribution as a function of normalized chord location and normalized span station for each of the pressure transducer locations on the respective experimental models. Computational results should be presented as a finely spaced function of chord location, but for quantitative comparative purposes, it is requested that the information also be extracted at the specified chordwise pressure sensor locations. For the RSW, BSCW and HIRENASD, there are respectively 4, 1, and 7 span stations. An example plot, using experimental data for the RSW, is shown in Figure 12. Integrated loads (lift coefficient, pitching moment coefficient and drag coefficient) should be provided. Note that these quantities will be compared only among the different computational results, except for the HIRENASD configuration, for which there is corresponding experimental data. Analysis results of the HIRENASD configuration should also include vertical linear displacements and twist angles at span stations corresponding to the displacement sensor locations.

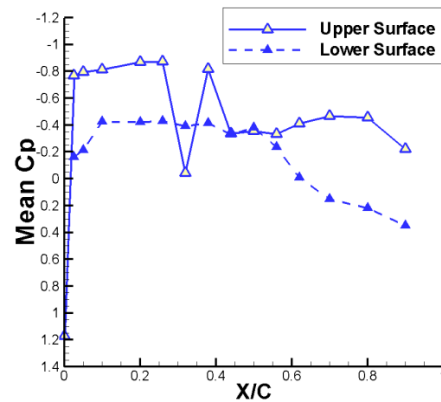


Figure 12. Steady experimental data sample results: Pressure coefficient at fixed static angle of attack, span station 2, $\eta = 0.588$, RSW experimental point 6E23.

Results from dynamic analyses should include the frequency response functions (FRFs) of the pressure coefficients due to displacement. These FRFs should be provided as the magnitude and phase calculated at a single frequency corresponding to the frequency of the excitation. The quantities should be calculated at each pressure transducer location. Computational results should be presented as a finely spaced function of chord location, but for quantitative comparative purposes, it is requested that the information also be extracted at the specified chordwise pressure sensor locations. Example plots, using experimental data for the RSW, are shown in Figure 13. FRFs of the integrated load coefficients (lift coefficient, pitching moment coefficient and drag coefficient) due to displacement should be calculated at the oscillation frequency. Time histories of the pressure coefficients should also be submitted for 3 sensor locations at each span station: two on the upper surface, ideally ahead and behind the shock, and one on the lower surface. Exact locations will be specified by the organizing committee, and will correspond to a subset of those sensor locations used to produce the transfer function information.

Definition of the reference displacement signal is different for the different configurations. The RSW and the BSCW are both oscillated in pitch; analyses of both configurations should use the angle of attack displacement as the excitation source in computing the frequency response functions. The reference signal for HIRENASD should be the vertical displacement at $x=1.24521$ m, $y=0.873034$ m, corresponding to the location of the wingtip accelerometer.

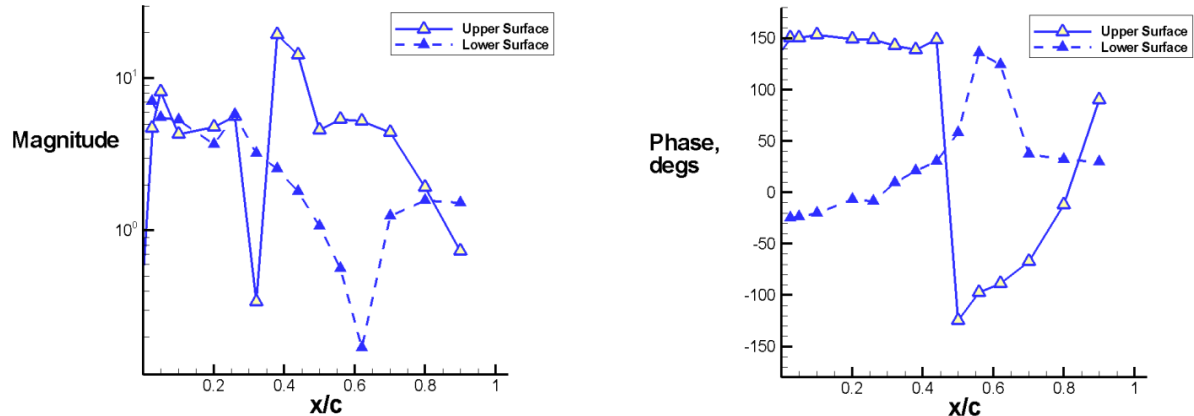


Figure 13. Dynamic analysis sample results using experimental data: Magnitude and phase of pressure coefficients due to angular deflection at 10 Hz, span station 2, $\eta = 0.588$, RSW experimental point 6E54.

Additional details for the required comparative data submissions are available on the project website (<https://c3.ndc.nasa.gov/dashlink/projects/47/>). Software for post processing the computational data and documents detailing the required data formatting for comparative data will also be posted there. The specifications for normalizations, units and sign conventions will also be provided.

9 CONCLUDING REMARKS

The objective in presenting this information is to solicit worldwide participation in assessment of the state of the art in aeroelastic computational methods. Members of the organizing committee for the Aeroelastic Prediction Workshop have examined existing configurations and data sets, selecting several which are hopefully of interest to and within the resource allocation of different organizations. Interested parties should visit the website for additional information, or contact a member of the organizing committee.

10 APPENDIX I: RESOURCES FOR PARTICIPANTS

- The website for the first Aeroelastic Prediction Workshop is <https://c3.ndc.nasa.gov/dashlink/projects/47/>
- HIRENASD website (German and English languages) <http://www.lufmech.rwth-aachen.de/HIRENASD/>
<https://heinrich.lufmech.rwth-aachen.de/index.php?lang=en&pg=home>
- Drag and High-Lift Prediction Workshops <http://aac.larc.nasa.gov/tsab/cfdlarc/aiaa-dpw/>
<http://hiliftpw.larc.nasa.gov/>

11 APPENDIX II: MICRO-ABSTRACT GUIDELINES

There are no written papers associated with this workshop; the presentations are not official AIAA presentations. Presentation of results at the workshop requires submission of a micro-abstract. A submitted abstract should be no more than one page in length. It should contain at least the following information: name(s), affiliation(s), corresponding author contact

information (mailing address, phone number and email address), test cases being analyzed, brief description of solver code(s), supplied grid(s) being used, brief description of other grid(s) being used, and structural model description where applicable. A sample micro-abstract can be downloaded from the workshop website.

12 REFERENCES

- ¹ Oberkampf, William L, and Trucano, Timothy G., "Verification and validation in computational fluid dynamics," SAND2002-0529, Sandia National Laboratories, Albuquerque, New Mexico, March 2002.
- ² Roy, Christopher J, and Oberkampf, William L, "A complete framework for verification, validation and uncertainty quantification in scientific computing," 48th AIAA Aerospace Sciences Meeting, Jan. 4-7, 2010, Orlando, Florida.
- ³ Anon., "Guide for the verification and validation of computational fluid dynamics simulations," American Institute of Aeronautics and Astronautics, AIAA-G-077-1998, Reston, VA, 1998.
- ⁴ Anon., "Assessment of experimental uncertainty with application to wind tunnel testing", American Institute of Aeronautics and Astronautics, S-071A-1999, Reston, VA, 1999.
- ⁵ Rahaim, C.P., Oberkampf, W. L., Cosner, R.R., and Dominik, D.F., "AIAA committee on standards for computational fluid dynamics- status and plans," AIAA-2003-844, 41st Aerospace Sciences Meeting, Jan. 6-9, 2003, Reno, Nevada.
- ⁶ Levy, David W., Zickuhr, Tom, Vassberg, John, Agrawal, Shreekanth, Wahls, Richard A., Pirzadeh, Shahyay, and Hemsch, Michael J., " Summary of data from the first AIAA CFD drag prediction workshop," AIAA-2002-0841, 40th AIAA Aerospace Sciences Meeting, Jan. 14-17, 2002, Reno Nevada.
- ⁷ Rumsey, C., Long, M., Stuever, R., and Wayman, T., "Summary of the First AIAA CFD High Lift Prediction Workshop," AIAA-2011-939 ,49th AIAA Aerospace Sciences Meeting including the New Horizons Forum and Aerospace Exposition, Orlando, Florida, Jan. 4-7, 2011
- ⁸ Green, Bradford, E., Czerwiec, Ryan, Cureton, Chris, Lillian, Chad, Kernazhitskiy, Sergey, Eymann, Tim, Torres, Jason, Bergeron, Keith, and Decker, Robert, "Evaluation of flow solver accuracy using five simple unsteady validation cases," AIAA-2011-29, 49th AIAA Aerospace Sciences Meeting, Jan. 4-7, 2011, Orlando, Florida.
- ⁹ Bennett, Robert M., and Edwards, John W., "An overview of recent developments in computational aeroelasticity," AIAA-98-2421.
- ¹⁰ Dowell, Earl, Edwards, John, and Strganac, Thomas, "Nonlinear Aeroelasticity," AIAA Journal of Aircraft, Vol 40, No 5, Sept.-Oct. 2003.
- ¹¹ Schuster, David, M, Scott, Robert C, Bartels, Robert E., Edwards, John W., and Bennett, Robert M., "A sample of NASA Langley unsteady pressure experiments for computational aerodynamics code evaluation," AIAA-2000-2602, AIAA Fluids 2000 Conference & Exhibit, June 19-22, 2000, Denver, Colorado.
- ¹² Yates, E. Carson, Jr, "AGARD standard aeroelastic configurations for dynamic response; Candidate configuration I.-wing 445.6," NASA TM-100492, Aug. 1987.
- ¹³ Ricketts, Rodney H., Sandford, Maynard C., Watson, Judith J., and Seidel, David A., "Geometric and Structural Properties of a rectangular supercritical wing oscillated in pitch for measurement of unsteady transonic pressure distributions," NASA TM-85763, Nov. 1983.
- ¹⁴ Ricketts, Rodney H., Sanford, Maynard C., Seidel, David A., and Watson, Judith J., "Transonic pressure distributions on a rectangular supercritical wing oscillating in pitch," NASA TM-84616, March 1983.

-
- ¹⁵ Ricketts, Rodney H., Sandford, Maynard C., Watson, Judith J. and Seidel, David A. "Subsonic and Transonic Unsteady and Steady-Pressure Measurements on a Rectangular Supercritical Wing Oscillated in Pitch," NASA TM 85765, Aug. 1984.
- ¹⁶ Bennett, Robert M., and Walker, Charlotte E., "Computational Test Cases for a Rectangular Supercritical Wing Undergoing Pitching Oscillations," NASA TM-1999-209130, April 1999.
- ¹⁷ Olsen, J. J., Lambourne, N.C., et al., "Compendium of unsteady aerodynamic measurements," AGARD R- 702, ISBN 92-835-1430-0, Aug. 1982.
- ¹⁸ Ruiz-Calavera, Luis, et al, "Verification and validation data for computational unsteady aerodynamics," RTO-TR-26, ISBN 92-837-1048-7, Report of the Applied Vehicle Technology Panel (AVT) Task Group AVT-010, Oct. 2000.
- ¹⁹ Schuster, David M., "Aerodynamic measurements on a large splitter plate for the NASA Langley Transonic Dynamics Tunnel," NASA TM-2001-210828, March 2001.
- ²⁰ Piatak, David J. and Cleckner, Craig S. Oscillating Turntable for the Measurement of Unsteady Aerodynamic Phenomenon, *Journal of Aircraft*, Vol 14, No. 1, Jan. –Feb. 2003.
- ²¹ Ballmann, J., Dafnis, A., Korsch, A., Buxel, C., Reimerdes, H-G, Brakhage, K-H, Olivier, H, Braun, C., Baars, A., and Boucke, A., "Experimental analysis of high Reynolds number aero-structural dynamics in ETW," AIAA 2008-841, 46th AIAA Aerospace Sciences Meeting & Exhibit, Jan. 7-10, 2008, Reno, Nevada.
- ²² Dafnis, A., Korsch, H., Buxel, C., Reimerdes, H.-G. "Dynamic Response of the HiReNASD Elastic Wing Model under Wind-Off and Wind-On Conditions", *International Forum on Aeroelasticity and Structural Dynamics*, IF-073, Stockholm. 2007.
- ²³ Ballmann, J., Boucke, A., Chen, B-H., Reimer, L., Behr, M., Dafnis, A., Buxel, C, Buesing, S., Reimerdes, H-G, Brakhage, K-H, Olivier, H., Kordt, M., Brink-Spalink, J., Theurich, F., and Buescher, A., "Aero-structural wind tunnel experiments with elastic wing models at high Reynolds numbers (HIRENASD-ASDMAD)", AIAA 2011-882, 49th AIAA Aerospace Sciences Meeting, Jan. 4-7, 2011, Orlando, Florida.
- ²⁴ Reimer, L., Braun, C., Chen, B.-H. Ballmann, J. "Computational Aeroelastic Design and Analysis of the HiReNASD Wind Tunnel Wing Model and Tests", *International Forum on Aeroelasticity and Structural Dynamics*, IF-077, Stockholm. 2007
- ²⁵ Reimer, L., Ballmann, J., Behr, M. "Computational Ananlysis of High Reynolds Number Aerostructural Dynamics (HiReNASD) Experiments" IFASD-2009-132, *International Forum on Aeroelasticity and Structural Dynamics*, Seattle Washington.
- ²⁶ Neumann, Jens, and Ritter, Markus, "Steady and unsteady aeroelastic simulations of the HIRENASD wind tunnel experiment," IFASD-2009-132, *International Forum on Aeroelasticity and Structural Dynamics*, Seattle Washington.
- ²⁷ Neumann, Jens, Nitzsche, Jens, and Voss, Ralph, "Aeroelastic analysis by coupled non-linear time domain simulation," RTO-MP_AVT-154, 2008.
- ²⁸ Mavriplis, D.J., Vassberg, J.C., Tinoco, E.N., Mani, M., Brodersen, O.P. Eisfeld, B., Wahls, R.A., Morrison, J.H., Zuckuhr, T., Levy, D., and Murayama, M., "Grid quality and resolution issues from the drag prediction workshop series," AIAA 2008-930, presented at the 46th AIAA Aerospace Sciences Meeting, Jan. 2008, Reno, Nevada.
- ²⁹ Samareh, J. A., "Discrete Data Transfer Technique for Fluid-Structure Interaction," AIAA Paper 2007-4309, 2007.